



# TiO<sub>2</sub> nanotube photonic crystal fabricated by two-step anodization method for enhanced photoelectrochemical water splitting



Kuili Liu, Gaoliang Wang, Ming Meng<sup>\*</sup>, Songling Chen, Jitao Li, Xianke Sun, Honglei Yuan, Lingling Sun, Nan Qin

School of Physics and Telecommunication Engineering, Zhoukou Normal University, Zhoukou 466001, China

## ARTICLE INFO

### Article history:

Received 6 June 2017

Received in revised form 7 July 2017

Accepted 8 July 2017

Available online 10 July 2017

### Keywords:

TiO<sub>2</sub> nanotube

Photonic crystal

Photoelectrochemical water splitting

Visible light absorption

## ABSTRACT

TiO<sub>2</sub> nanotube photonic crystal (TiO<sub>2</sub> TSANTPC) is successfully fabricated via a facile two-step anodization method. The TiO<sub>2</sub> TSANTPC exhibits a strong light absorption over a broad visible range. When it was used as a photoanode in photoelectrochemical (PEC) water splitting, the photocurrent density of the TiO<sub>2</sub> TSANTPC was identified to be 1.1 mA/cm<sup>2</sup> at 0.22 V vs. Ag/AgCl electrode with Faradic efficiency of 100%, which is approximately 4.8-fold enhanced over pristine TiO<sub>2</sub> nanotube. These findings contribute to further enhancement of the PEC performance of TiO<sub>2</sub>-based photoelectrode.

© 2017 Elsevier B.V. All rights reserved.

## 1. Introduction

One-dimensional (1D) semiconductor nanostructures have been capturing significant attention because of the unique physical properties and their extensive applications in photodegradation [1–3], water splitting and purification [4–7], supercapacitors [8], etc. Among the 1D semiconductor nanostructures utilized in photoelectrochemical (PEC) water splitting, TiO<sub>2</sub> nanotube arrays (TiO<sub>2</sub> NTAs) are considered as viable competitors owing to their fascinating features such as vertically aligned structure and large surface areas, all of which are beneficial for PEC performance enhancement [4–6,9,10]. Nevertheless, the TiO<sub>2</sub> NTAs suffer from some disadvantages, including large band gap energy, strong surface reflection and weak visible light harvesting [11–14]. To tackle this problem, several effective strategies have been proposed, for instance, band engineering [6], element doping [15] and introducing of oxygen deficiency [4,13], etc. Despite these efforts, the solar-to-hydrogen conversion efficiency of TiO<sub>2</sub> NTAs have remained extremely low and an effective approach to enhance visible light absorption is yet urgently demanded.

Recently, the hierarchical TiO<sub>2</sub> NTAs with top layer serving as photonic crystals (TiO<sub>2</sub> NTPCs) have been extensively investigated, because the periodical top nanoring layer can trap visible light, thus improving PEC performance [9–11,16]. Unfortunately, the TiO<sub>2</sub> NTPCs show multiabsorption peaks in UV and visible-light

regions. To maximize the light trapping, a strong light absorption over a broader visible-light range is preferred. In this work, we demonstrate that the nanostructural defects of TiO<sub>2</sub> NTPCs lead to a strong light absorption over a broader visible-light range instead of multiabsorption peaks, which indicates that it may utilize visible light much better. When used as a photoanode, an impressive photocurrent of 1.1 mA/cm<sup>2</sup> was achieved under white light irradiation, which is 4.8 times of that of TiO<sub>2</sub> NTAs. This work contributes to further enhancement of PEC performance of TiO<sub>2</sub>-based photoelectrodes, and this film can also potentially be employed other fields such as dye-sensitized solar cells.

## 2. Materials and methods

The source of chemicals/materials have been given in the [Supplementary data \(SD\)](#). The TiO<sub>2</sub> NTPCs with nanostructural defects (TiO<sub>2</sub> TSANTPCs) were synthesized by two-step anodization method. Before anodization, Ti substrates were ultrasonically cleaned in ethanol and deionized water, and then dried in a Ar stream. The anodization was performed in a glycol electrolytes containing 0.3 wt% NH<sub>4</sub>F and 2 vol% deionized water using a conventional two-electrode configuration, with the Ti substrate being the working electrode, Pt mesh the counter electrode. In the first-step anodization, TiO<sub>2</sub> NTAs were prepared at 60 V for 1 h. After ultrasonic removal of the NTAs layer, the textured Ti substrate with nanoconcaves was obtained. Subsequently, the textured Ti substrate was subjected the second-step anodization at 30 V for

<sup>\*</sup> Corresponding author.

E-mail address: [mengmingfly@163.com](mailto:mengmingfly@163.com) (M. Meng).

30 min, then 35 V for 30 min and finally 40 V for 30 min. After the two-step anodization, the TiO<sub>2</sub> TSANTPCs were annealed at 450 °C for 3 h.

The characterizations were performed on FE-SEM (Hitachi S4800), FE-TEM (JEOL-2100), XRD (Philips, Xpert), XPS (PHI5000 VersaProbe). The UV–vis absorption spectra were acquired on a VARIAN Cary5000 spectrophotometer. The PEC performances were evaluated in a 1 M NaOH (pH = 13.6) electrolyte using three electrodes configuration, with the TiO<sub>2</sub> samples being the working electrode, Pt mesh the counter electrode, and Ag/AgCl (3 mol L<sup>-1</sup> KCl-filled) the reference electrode. A 500 W Xe lamp illuminated the TiO<sub>2</sub> with a power of 100 mW/cm<sup>2</sup>. An Ocean Optics oxygen sensor system equipped with a FOXO probe (NeoFox Phase Measurement System) was employed to determine the amount of evolved O<sub>2</sub>.

### 3. Results and discussion

The morphologies of the TiO<sub>2</sub> samples were examined by FE-SEM. Fig. 1a and b shows that the TiO<sub>2</sub> NTAs were vertically aligned on the Ti substrate, with average diameter of about 180 nm, wall thickness of around 20 nm and average length of 7 μm. After ultrasonic treatment, the textured Ti substrate with hexagonal nanoconcaves were obtained (bottom right inset of Fig. 1b). After the second-step anodization, the TiO<sub>2</sub> TSANTPCs were directly grown from the textured Ti substrate. Fig. 2c displays a clear periodical hexagonal nanoring structure on the top. It is worthy noted that some of them possess a random nanostructural defects as highlighted by the red arrows. The typical FE-SEM image and schematic structure clearly show an average hexagon diameter of around 180 nm, and a frame thickness of about 10 nm (Fig. 1d and e). The cross-sectional FE-SEM images confirm that TiO<sub>2</sub> TSANTPCs consist of the top-nanoring layer and the bottom nanotube nanostructures, with top-layer thickness being about 30 nm and a nanotube length of about 7 μm (Fig. 1f and g).

The TiO<sub>2</sub> NTAs and the TiO<sub>2</sub> TSANTPCs were further investigated by FE-TEM. Both samples exhibit a tightly packed tubular nanostructure (Fig. 2a and e). The HR-TEM images display an identical lattice fringes with an interplanar distance of 0.35 nm, belonging to the d-spacing of the (1 0 1) plane of the anatase TiO<sub>2</sub> (Fig. 2b and f), which also confirmed by the fast Fourier transform (FFT) on the selected area bounded by the red dashed-line box and

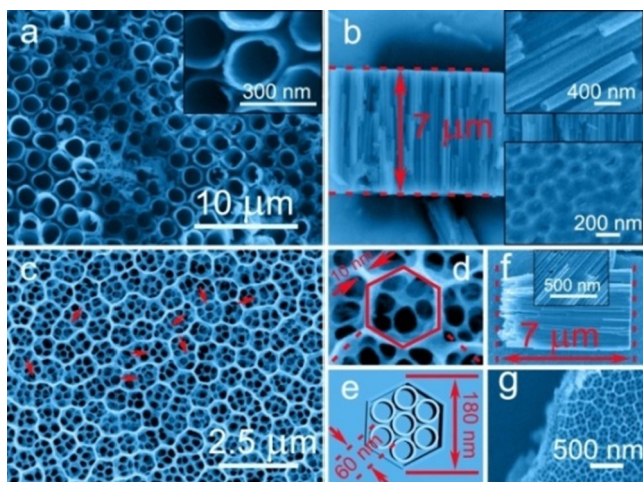


**Fig. 1.** (a, b) FE-SEM images of the TiO<sub>2</sub> NTAs; The bottom right inset of (b) shows the FE-SEM image of Ti substrate surface after ultrasonic removal of the NTAs layer. (c, d) FE-SEM images of the TiO<sub>2</sub> TSANTPCs (e) Schematic illustration of the TiO<sub>2</sub> TSANTPC. (f, g) SEM images: cross section and partial cross-section view of the TiO<sub>2</sub> TSANTPCs.

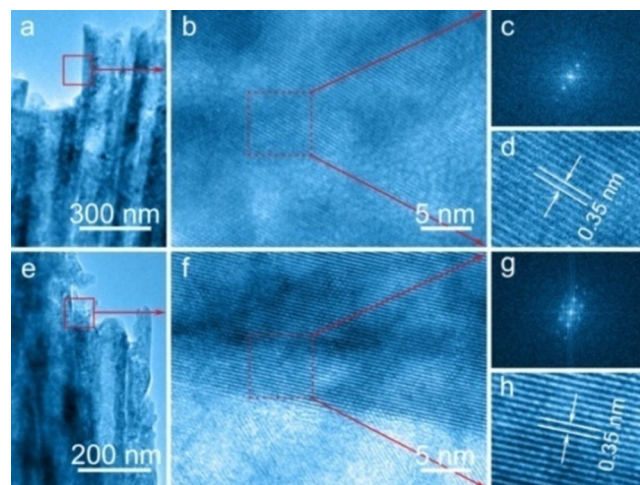


**Fig. 2.** (a, b) FE-TEM images of the TiO<sub>2</sub> NTAs. (c, d) Fast-Fourier-transform-filtered (FFTF) and inverse fast-Fourier-transform-filtered (IFFTF) TEM images recorded from area bounded by the red dashed-line box in Fig. 2b. (e, f) FE-TEM images of the TiO<sub>2</sub> TSANTPCs. (g, h) FFTF and IFFTf TEM images recorded from area bounded by the red dashed-line box in Fig. 2f. (For interpretation of the references to colour in this figure legend, the reader is referred to the web version of this article.)

the inverse fast Fourier transform (IFFT) (Fig. 2c, d, g and h). These results clearly demonstrate that there is no obvious microstructure difference between the TiO<sub>2</sub> NTAs and the TiO<sub>2</sub> TSANTPCs. The element mapping images of the TiO<sub>2</sub> NTAs and the TiO<sub>2</sub> TSANTPCs indicate that the major elements of Ti and O distribute uniform (Fig. S1a and b). Except for Ti and O elements, no other compositions are detected, indicating that both samples are enough pure. XPS analysis results further confirm this point (Fig. S1c–e). The growth mechanism of the TiO<sub>2</sub> NTAs and the TiO<sub>2</sub> TSANTPCs was clearly discussed based on chemistry concept as shown by the Fig. S2 in the SD.

Fig. 3a shows that all the diffraction peaks match well with those of the anatase TiO<sub>2</sub> phase (JCPDS card No. 21-1272) and Ti metal phase, revealing that both samples are pure anatase TiO<sub>2</sub>. The UV–visible absorption spectra are shown in Fig. 3b. It can be seen that both samples show fairly high absorption at wavelength shorter than 390 nm and the absorption decrease rapidly at about 400 nm, which was assigned to the intrinsic band-to-band adsorption of anatase TiO<sub>2</sub>. In addition, the band gaps of the both samples, estimated from the main absorption edge of the profile, are almost identical (about 3.2 eV). Compared with TiO<sub>2</sub> NTAs, the TiO<sub>2</sub> TSANTPCs have a strong light absorption over a broader visible-light range (400–800 nm). This optical adsorption property was also different from the multiabsorption peaks of TiO<sub>2</sub> NTPCs without nanostructural defects, which indicates that TiO<sub>2</sub> TSANTPCs may utilize visible light much better. Since they have the same microstructure and crystal structure, the stronger absorption can be attributed to the featured top photonic periodic nanoring structure with nanostructural defects, which may result in stronger scattering light [17]. In addition, the unique hierarchical structural may serve as a Fabry-Perot resonant cavity, incident light reflects several times, and thus promoting the light absorption [16]. The BET surface areas of the TiO<sub>2</sub> NTAs and TiO<sub>2</sub> NTAs TSANTPCs are 26.62 and 32.05 m<sup>2</sup> g<sup>-1</sup>, respectively (Fig. S3 in the SD). These results imply that the TiO<sub>2</sub> TSANTPCs have a large potential in PEC water splitting applications.

The PEC performance of the TiO<sub>2</sub>-based photoanodes were performed in three-electrode electrochemical cell configuration. Fig. 3c displays the current versus voltage (*J*-*V*) curves of the TiO<sub>2</sub> NTAs and the TiO<sub>2</sub> TSANTPCs. The dark current densities of both samples were almost negligible. Under illumination, the photocur-

Download English Version:

<https://daneshyari.com/en/article/5463257>

Download Persian Version:

<https://daneshyari.com/article/5463257>

[Daneshyari.com](https://daneshyari.com)